

Kinematic Analysis of WMR Tracked by a Camera Vision System

Hasan M. Alwan
Mechanical Eng. Dep.
University of Technology

Qasim A. Atiyah
Mechanical Eng. Dep.
University of Technology

Hussein A. Hasan
Mechanical Eng. Dep.
University of Technology
eng.hussein.msc@gmail.com

Abstract

This paper presents a study of a nonholonomic differential drive wheeled mobile robot (WMR) of the type (BOE-Bot). In this paper, two aims are presented: the first is the study of the WMR movement on a specific trajectories to get the desired goals positions and the second is the evaluation of the kinematic performance factor of the WMR movement. The kinematic model of the robot movement in terms of the robot wheels velocity is studied by making the robot to move on the desired trajectories. The determination of the actual robot centre position in two dimensions (X) and (Y) is done by tracking the movement of a red point located above the robot by using a fixed camera attached to the ceiling. The position error between the theoretical and actual WMR position vectors is studied and calculated in global and local coordinates' frames. The values of the position error percentage ratios when the robot moved on a (S-shape) trajectory were higher than its values when the robot moved on a (straight-line) trajectory because of the existence of a gyroscopic torque resulted from the WMR circular movement around an axis perpendicular to the axis of the WMR wheels rotation. Finally, the kinematic performance factor of the WMR movement is evaluated depending on the position error in the global coordinate.

Keywords: Mobile Robot, Kinematic Analysis, Localization, Position Error.

1. Introduction

The study of robots acquired a great interest in the last few years, due to their extensive benefits and applications in several fields (scientific, industrial, health, military, etc.). These robots differ with each other in their movement, mobility and applications that are used for it.

For several decades, robots have been developed to move automatically from place to place and they are called as mobile robots [1], so, it can say that the mobile robots are mechanisms that can move from one place to another autonomously, (i.e., without assistance from external human operators). Mobile robots cover robots that roll, walk, fly or swim.

WMR is a robot capable to move on a surface solely by actuation of wheel assemblies mounted

on the robot and in contact with the surface. The wheel assembly is a device, which delivers or permits relative motion between its mount and a surface on which it is intended to have a single point of rolling contact [2].

This paper studies the differential drive WMR movement on specific trajectories to reach a specific position and presents the evaluation of the kinematic performance factor of this movement.

In the beginning, the robot is moved on a specific trajectory. The robot can be localized at any point of its movement using several methods such as ultrasonic sensor [3, 4], GPS with Odometer [5], infrared [6] and cameras [7, 8, 9, 10, 11 and 12]. However, it differ with each other according to the robot movement case.

In this paper, we have a WMR should be indoor localized and it moves on small area, so, the GPS system cannot be used because it used for WMR outdoor localization where it moves on large areas. The ultrasonic and infrared sensors is not quite accurate to be used here. The camera vision system is the best choice to be used for indoor WMR localization.

There are different types of the camera vision system depending on the camera movement. Some of researchers used a fixed camera [9, 10, 11, 12] and the others used a camera mounted on the mobile robot and rotated to different directions [7, 8]. In this paper, a fixed camera attached to the ceiling is used to localize the robot position vector because the camera is placed at a position that it is allowed to observe the task space and the robot.

Since the camera is not visible to any motion, the geometric relation between the task space and the camera does not change. However, the robot movement can impede the clear view of the task space of the camera and this obstruction can make severe decreasing in the performance or even some instability issues [13].

When the robot is moved on the proposed trajectories it deviates from the desired trajectory. This deviation caused a position error. This error is studied and calculated in global and local coordinates' frames. Finally, the relation between the position error in the global coordinates frame and the kinematic performance factor of the WMR movement is derived.

2. Kinematic Model of WMR

The differential drive WMR as shown in Figure (1) comprised of a vehicle with couple of driving wheels installed on one axis and a passive self-adjusted-supporting wheel, which carries the mechanical structure. Two actuators of the type (servomotors) separately drive the two driving wheels.

It is assumed that the mobile robot is composed of a rigid frame equipped with no deformable wheels and that they are moving on a horizontal plane.

Both driving wheels have the same radius r and the distance between them is $2D$. The centre of mass of the mobile robot is assumed to locate at point m [14].

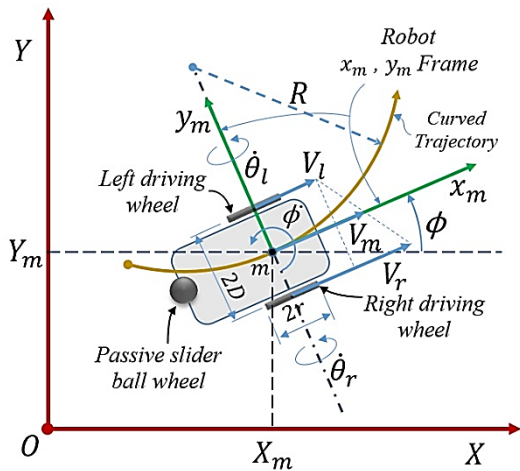


Figure 1: Kinematic structure of differential drive WMR.

The position vector of the robot centre in the global coordinate frame OXY can be completely specified by three generalized coordinates $\zeta = [X_m \ Y_m \ \phi]^T$, where X_m and Y_m are the coordinates of the robot centre point m in the global coordinate frame and ϕ is the orientation of the local frame mx_my_m attached to the robot platform according to the global coordinate system.

The following assumptions are taken in consideration:

1. Robot wheels are rolling without slipping.
2. The centre of mass is located at the axis of the wheels rotation.

The angular velocities of the left and right wheels are $\dot{\theta}_l$ and $\dot{\theta}_r$ respectively. The linear velocities of the left and right robot wheels are V_l and V_r respectively.

V_m and $\dot{\phi}$ are respectively the linear and angular velocities of the WMR centre m and it can be calculated using the following relations [15]:

$$V_m = \frac{1}{2}(V_r + V_l) \quad (1)$$

$$\dot{\phi} = \frac{1}{2D}(V_r - V_l) \quad (2)$$

Velocity components \dot{X}_m and \dot{Y}_m are given by:

$$\dot{X}_m = V_m \cos \phi \quad (3)$$

$$\dot{Y}_m = V_m \sin \phi \quad (4)$$

So, the kinematic model of the WMR can be described by the following relation [15]:

$$\begin{bmatrix} \dot{X}_m \\ \dot{Y}_m \\ \dot{\phi} \end{bmatrix} = \begin{bmatrix} \left(\frac{r}{2}\right) \cos \phi & \left(\frac{r}{2}\right) \cos \phi \\ \left(\frac{r}{2}\right) \sin \phi & \left(\frac{r}{2}\right) \sin \phi \\ \frac{r}{2D} & -\frac{r}{2D} \end{bmatrix} \begin{bmatrix} \dot{\theta}_r \\ \dot{\theta}_l \end{bmatrix} \quad (5)$$

The non-slipping condition does not allow the generalized velocities \dot{X}_m, \dot{Y}_m , and $\dot{\phi}$ to take arbitrary values. Due to the non-slipping condition, the generalized coordinates are constrained by the equations (3) and (4). These constraints are not integrable. Eliminating the velocity V_m in these equations gives:

$$\dot{X}_m \sin \phi - \dot{Y}_m \cos \phi = 0 \quad (6)$$

or in matrix notation:

$$[\sin(\phi) \quad -\cos(\phi)] \begin{bmatrix} \dot{X}_m \\ \dot{Y}_m \end{bmatrix} = 0 \quad (7)$$

3. Position Error

The goal to be achieved is to follow the robot theoretical trajectory, defined as $\zeta_{th} = [X_{mth} \ Y_{mth} \ \phi_{th}]^T$. The position error of the robot centre $e = [e_x \ e_y \ e_\phi]^T$ is given in the local coordinate system of the robot as shown in Figure (2) can be evaluated depending on the theoretical position vector ζ_{th} and the actual position vector $\zeta_{act} = [X_{mact} \ Y_{mact} \ \phi_{mact}]^T$ using the following equation [16]:

$$\begin{bmatrix} e_x \\ e_y \\ e_\phi \end{bmatrix} = \begin{bmatrix} \cos \phi_{act} & \sin \phi_{act} & 0 \\ -\sin \phi_{act} & \cos \phi_{act} & 0 \\ 0 & 0 & 1 \end{bmatrix} \begin{bmatrix} X_{mth} - X_{mact} \\ Y_{mth} - Y_{mact} \\ \phi_{th} - \phi_{act} \end{bmatrix} \quad (8)$$

Where e_x gives the error in the robot driving direction, e_y gives the error in the lateral direction and e_ϕ gives the error in the robot orientation.

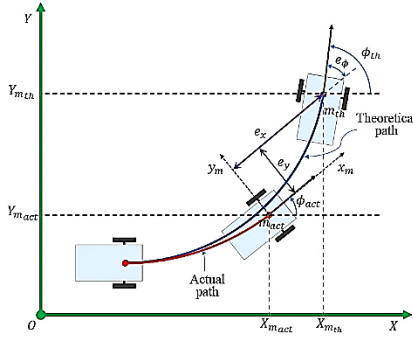


Figure 2: The position error in the local coordinate frame.

4. Kinematic Performance Factor

The kinematic performance factor evaluation requires the calculation of the position error ratio $r_e = [r_x \ r_y \ r_\phi]^T$ in the global coordinates.

The position error ratio is the absolute difference error between the theoretical ζ_{th} and actual ζ_{act} robot position vector of the robot centre of mass m divided by the linear S_x (or angular S_ϕ) distance, which is travelled by the robot.

The position error ratio can be evaluated using the following functions:

$$r_x = \frac{|x_{mth} - x_{mact}|}{S_x} * 100 \% \tag{9}$$

$$r_y = \frac{|y_{mth} - y_{mact}|}{S_x} * 100 \% \tag{10}$$

$$r_\phi = \frac{|\phi_{th} - \phi_{act}|}{S_\phi} * 100 \% \tag{11}$$

Now, the kinematic performance factor of the WMR trajectory tracking $\Gamma = [\Gamma_x \ \Gamma_y \ \Gamma_\phi]^T$ can be evaluated depending on position error ratio r_e from the following equation:

$$\Gamma = \begin{bmatrix} \Gamma_x \\ \Gamma_y \\ \Gamma_\phi \end{bmatrix} = 100\% - \begin{bmatrix} r_x \\ r_y \\ r_\phi \end{bmatrix} \tag{12}$$

5. Experimental part

The WMR used in this work is a differential drive WMR of the type (BOE-Bot) WMR, as shown in Figure (3). This type of WMR is used around the world by students, educators and hobbyists. It has the following features:

1. Programmable: PBASIC is easy to learn and introduces concepts found in most programming languages.
2. Autonomous: touch, light and infrared sensors let the Boe-Bot navigate on its own.
3. Lightweight: The total weight of this WMR is 300 g without batteries.

- The dimensions of this WMR are as follows:
1. Metal body is 127 mm long by 82.55 mm wide.
 2. Large plastic wheels are 66.04 mm diameter and 7.62 mm thick at the thickest part (rim).
 3. The small wheel is 25.4 mm diameter.
 4. The metal is 1.52 mm thick.

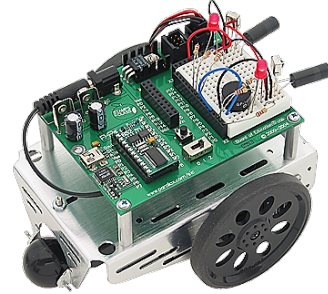


Figure 3: BOE-Bot WMR.

The WMR is moved on two types of trajectories as shown in Figure (4). The first is a (straight-line trajectory) and the second is an (S-shape trajectory), which is a half-circles connected with each other.

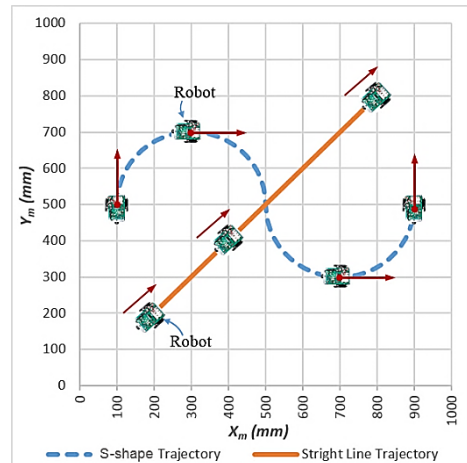


Figure 4: The trajectories types

The determination of the actual robot centre position in two dimensions (X) and (Y) is done by tracking the movement of the red point located above the robot by using a fixed camera attached to the ceiling of the type (USB 2.0 webcam "YUY2_640x480" pixel).

The camera takes several consecutive snapshots at specific periods of time during the robot movement, and then image processing is done by using MATLAB software to find the coordinates of the red point for each snapshot, which represents the current robot centre position.

The calibration of the camera is done by locating (X-axis) and (Y-axis) on the board using the camera by lifting the board of trajectories to a height of ($z = 110 \text{ mm}$), which is the height of the red point on the WMR, which is followed by

the camera to locate the experimental WMR centre position, as shown in Figures (5) and (6).

The axes of the board should be matched with the axes of the camera picture to get the experimental WMR centre position more accurate

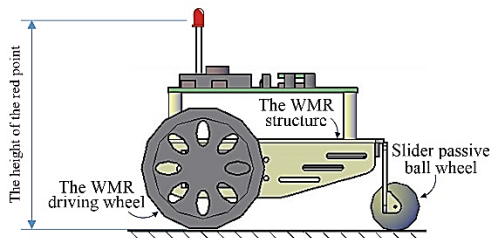


Figure 5: Side view of the WMR.

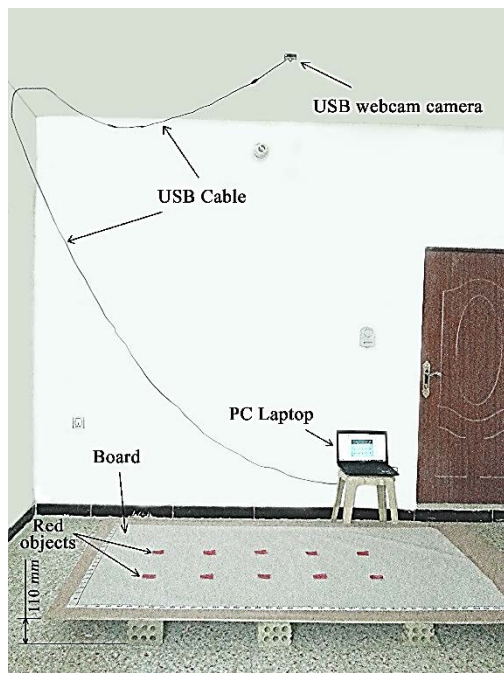


Figure 6: Lifting the board.

A simple function can be used to convert the dimension resulted from division of the real dimension in millimetres over the measured dimension in pixels.

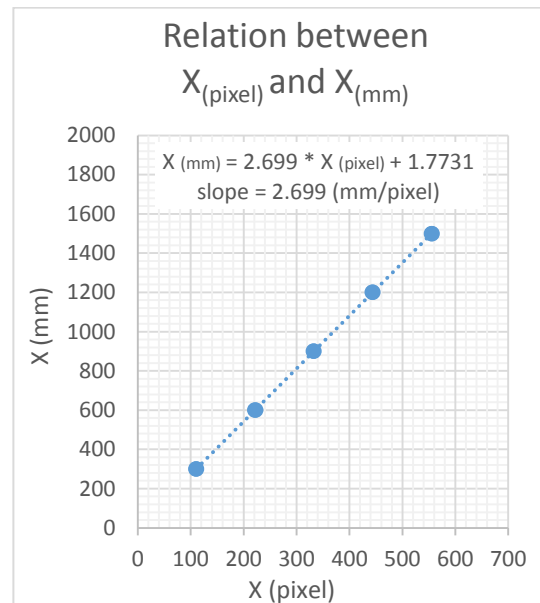
First, a calibration for the dimensions must be performed by putting some red objects on the board in known positions and getting the reading of their positions using the camera, as shown in Figure (7).

The values of the camera readings of the red objects centres positions and the values of the actual centres positions of these objects are used to draw the relations between the readings (in pixel units) and the actual positions (in millimetres units) as shown in figures (8A) and (8B).

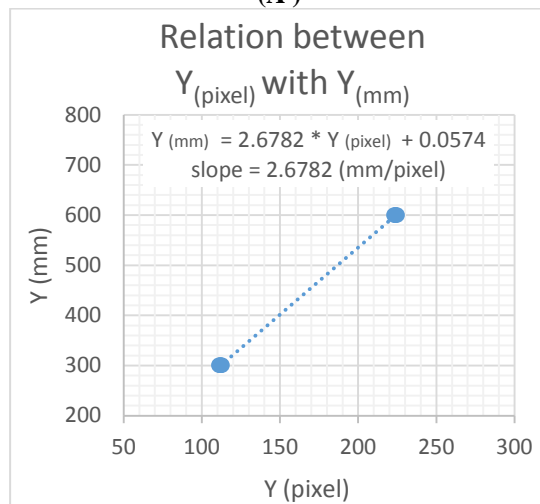
Later, these relations were added to the program of the camera image processing on the computer to edit the coordinates and convert the positions readings from pixels units to millimetres units.



Figure 7: Positions readings (in pixel units) and actual positions (in millimetres units) of red objects.



(A)



(B)

Figure 8: The relations between the positions readings (in pixel units) and the actual positions (in millimetres units) of the red objects

6. Experimental Results:

The values of the WMR position error ratio and the kinematic performance factor of the

WMR are evaluated at any point of the desired trajectories using equations, which are previously mentioned.

6.1. Results of Straight-Line Trajectory

The theoretical trajectory is a straight line from (200,200,0) to (800,800,0) and its equation is $(Y_{mth} = X_{mth})$.

The actual trajectory is not a linear trajectory, but a curved trajectory. Because of the robot wheels rotation at constant speed, so, the robot should move on circular trajectory.

The values of $(X_{mth}, Y_{mth}, X_{mact}$ and $Y_{mact})$ can be used to plot the theoretical and actual trajectories as shown in Figure (9).

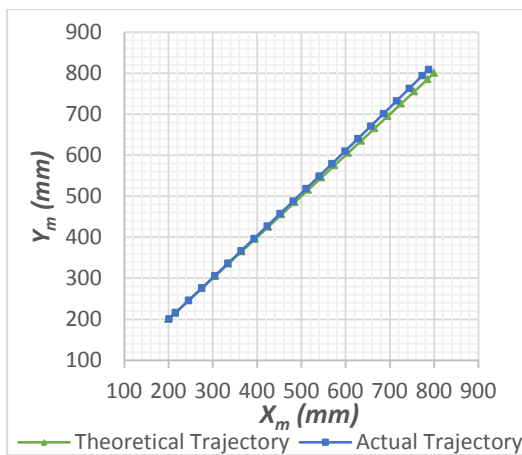


Figure 9: the actual and theoretical trajectories.

The position error ratio and kinematic performance factor values of the WMR movement on the straight-line trajectory are evaluated by using equations (9, 10, 11 and 12) to plot the variation of these values with time of the WMR movement as shown in Figure (10) and Figure (11).

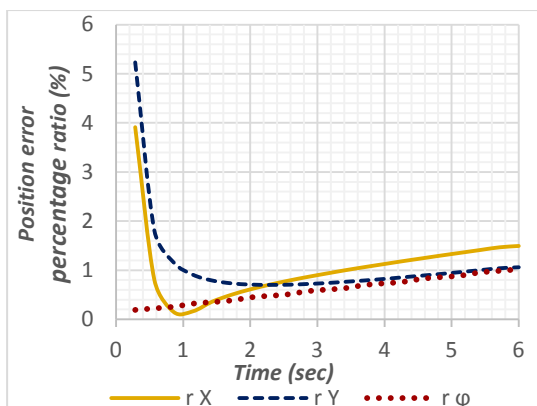


Figure 10: The position error percentage ratio with respect to time.

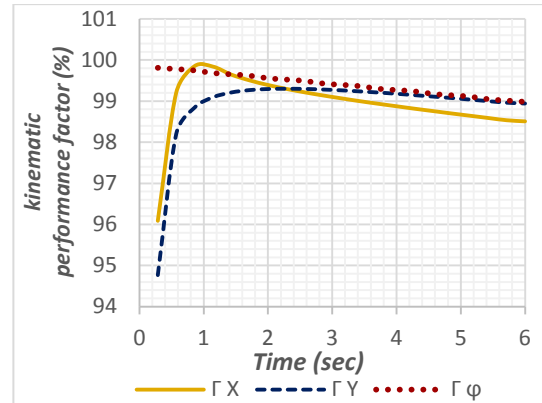


Figure 11: The kinematic performance factor with respect to time.

6.2. Results of the S-Shape Trajectory

The theoretical trajectory is a semi-circular trajectory, the equation of the first circular-half is:

$$Y_m = \sqrt{40000 - (X_m - 300)^2} + 500$$

The equation of the second circular-half is:

$$Y_m = -\sqrt{40000 - (X_m - 700)^2} + 500$$

The values of $(X_{mth}, Y_{mth}, X_{mact}$ and $Y_{mact})$ can be used to plot the theoretical and actual trajectories as shown in Figure (12).

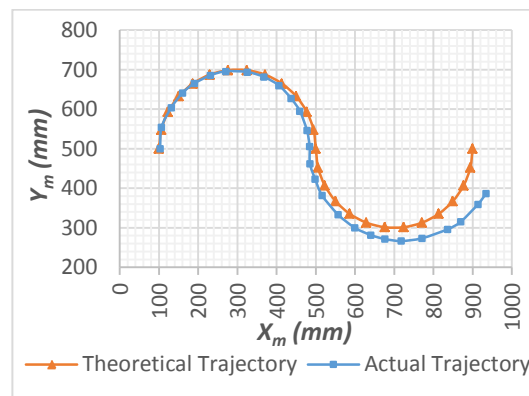


Figure 12: The actual and theoretical trajectories.

The kinematic performance factor of the WMR trajectory tracking Γ and its parameters are evaluated by using equations (9, 10, 11 and 12) to plot the variation of these values with time of the WMR movement as shown in Figure (13) and Figure (14).

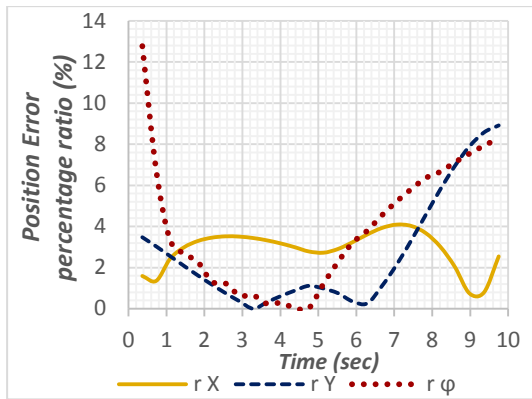


Figure 13: The position error percentage ratio with respect to time.

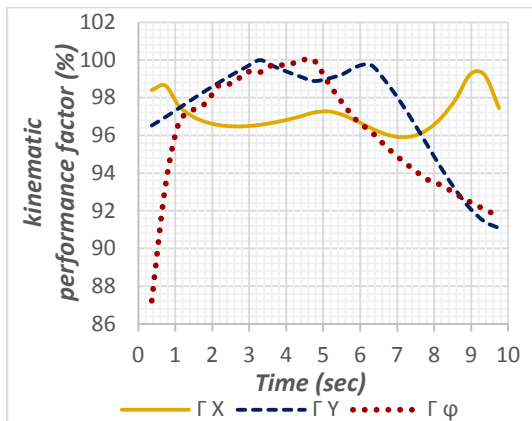


Figure 14: The kinematic performance factor with respect to time.

7. Conclusions:

There are position errors between the actual and theoretical WMR movement on the desired trajectories. The experimental results showed the following conclusions:

1. The position error ratios of the WMR trajectory tracking when the WMR moved on the straight-line trajectory was ranging between (0.15 % – 1.493 %).
2. The position error ratios of the WMR trajectory tracking when the WMR moved on the S-shape trajectory was ranging between (0.005 % – 8.914 %). This ratio is different from the ratio of the straight-line trajectory, because there was a gyroscopic torque. This torque was existed because of the WMR circular movement around an axis, which is perpendicular to the axis of the WMR wheels rotation.
3. The position error was resulted from many reasons, such as: the initial position error occurred because there are a few milliseconds separating between the movement of the two wheels, and the error in camera readings of WMR centre position which was ranging between $\pm (1 - 2)$ mm.

References:

- [1] A. Kelly “Mobile Robotics; Mathematics, Models, and Methods”. Cambridge University Press, (2013).
- [2] Patrick F. Muir and Charles P. Neuman “Kinematic Modeling of Wheeled Mobile Robots” Department of Electrical and Computer Engineering, The Robotics Institute, Camegie-Mellon University, Pittsburgh, Pennsylvania, USA, June (1986).
- [3] M. Peca "Ultrasonic Localization of Mobile Robot Using Active Beacons and Code Correlation". Communications in Computer and Information Science Research and Education in Robotics - EUROBOT 2009, pp. 116-130. DOI: 10.1007/978-3-642-16370-8_11. (2010).
- [4] S. Naveed and N. Y. Ko “Analysis of Indoor Robot Localization Using Ultrasonic Sensors”. International Journal of Fuzzy Logic and Intelligent Systems Vol. 14, No. 1, pp. 41-48, DOI: 10.5391/IJFIS.2014.14.1.41, March (2014).
- [5] Ch. K. Mishra, B.K. Mishra. J. S. Jebakumar “EKF Based GPS/Odometer Data Fusion for Precise Robot Localization in Outdoor Environment”. Journal of Mechanical and Civil Engineering, Vol. 11, No. 2, Ver. 4, PP 70-75, March – April (2014).
- [6] J. Bae, S. Lee and J. B. Song “Use of coded infrared light for mobile robot localization”. Journal of Mechanical Science and Technology Vol. 22, No. 7, pp. 1279-1286. DOI: 10.1007/s12206-008-0320-1. (2008).
- [7] E. Krotkov “Mobile Robot Localization Using a Single Image”. International Conference on Robotics and Automation. DOI: 10.1109/robot.1989.100108. May (1989).
- [8] F. Chenavier and J. L. Crowley “Position Estimation for a Mobile Robot Using Vision and Odometry”. IEEE International Conference on Robotics and Automation. Vol. 3, pp. 2588-2593, DOI: 10.1109/ROBOT.1992.220052, May (1992).
- [9] W. E. Dixon, D. M. Dawson, E. Zergeroglu and A. Behal “Adaptive Tracking Control of a Wheeled Mobile

- Robot via an Uncalibrated Camera System". IEEE Transactions on Systems, Man and Cybernetics Part (B): Cybernetics, Vol. 31, No. 3, pp. 341-352, DOI: 10.1109/3477.931519, June (2001).
- [10] Ch. Ch. Chia et al "Cooperative Surveillance System with Fixed Camera Object Localization and Mobile Robot Target Tracking". Advances in Image and Video Technology, Vol. 5414 of the series Lecture Notes in Computer Science, pp. 886-897, DOI: 10.1007/978-3-540-92957-4_77, January (2009).
- [11] A. Zdešar, I. Škrjanc and G. Klančar "Visual Trajectory-Tracking Model-Based Control for Mobile Robots". International Journal of Advanced Robotic Systems, Vol. 10, No. 9, DOI: 10.5772/56757, September (2013).
- [12] H. Chen, Sh. Ding, X. Chen, L. Wang, Ch. Zhu and W. Chen "Global Finite-time Stabilization for Nonholonomic Mobile Robots Based on Visual Servoing". International Journal of Advanced Robotic Systems, Vol. 11, No. 11, pp. 1-13, DOI: 10.5772/59307, November (2014).
- [13] T. Tepe, Prof. Dr. Henk Nijmeijer and Dr. Dragan Kostić "Mobile Robot Navigation Using Visual Servoing ". M.Sc. Thesis (2010).
- [14] K. Wang "Near-Optimal Tracking Control of a Nonholonomic Mobile Robot with Uncertainties". International Journal of Advanced Robotic Systems, Vol. 9, No. 3, pp. 1-11. DOI: 10.5772/51189, September (2012).
- [15] S. G. Tzafestas "Introduction to Mobile Robot Control". 1st Edition, Elsevier, (2014).
- [16] S. Blažič and M. Bernal "Trajectory Tracking for Nonholonomic Mobile Robots based on Extended Models". IFAC Proceedings Volumes Vol. 44, No. 1 pp. 5938-5943, DOI:10.3182/20110828-6-it-1002.01237, January (2011).

تحليل كينماتيكي لحركة روبوت متنقل مُتَّبَع بوساطة نظام رؤية بالكاميرا

حسين عبد الهادي حسن
قسم الهندسة الميكانيكية
الجامعة التكنولوجية

قاسم عباس عطية
قسم الهندسة الميكانيكية
الجامعة التكنولوجية

حسن محمد علوان
قسم الهندسة الميكانيكية
الجامعة التكنولوجية

الخلاصة

تم دراسة روبوت متنقل ذو عجلتين مختلفة الدفع من نوع (BOE-Bot). تعرّض البحث الى هدفين هما دراسة حركة الروبوت على مسارات معينة للوصول الى الموقع المطلوب وحساب معامل الأداء الكينماتيكي. تمت دراسة النموذج الكينماتيكي لحركة الروبوت بدون تأثير القوى بدلالة سرعة عجلات الروبوت عن طريق تحريك الروبوت على المسارات المطلوبة. عملية اخذ القراءات لموقع الروبوت في البعدين (X) و (Y) تمت عن طريق تتبع حركة نقطة حمراء فوق الروبوت بوساطة كاميرا مثبتة بالسقف. كما تمت دراسة الخطأ بين الموقع النظري والحقيقي للروبوت وتم حسابه في محاور الروبوت والمحاور العامة. قيم النسب المئوية للخطأ بموقع الروبوت عند حركته على مسار (شكل (S)) كانت أعلى من قيمها عند حركة الروبوت على مسار (خط مستقيم) بسبب وجود عزم جايروسكوبي ناتج من حركة الروبوت الدائرية حول محور عمودي على محور دوران العجلات. ثم تم حساب معامل الأداء الكينماتيكي لحركة الروبوت بالاعتماد على الخطأ بموقع الروبوت في المحاور العامة.